Numerical and graphical description on the ion motions in a Penning trap for mass measurements

Y.L. Sun[a,b], Y.L. Tian[a], W.X. Huang[a,*], J.Y. Wang[a], Y.S. Wang[a], J.M. Zhao[a], Y. Wang[a]

[a] *Institute of Modern Physics, Chinese Academy of Sciences, Lanzhou 730000, China*
[b] *University of Chinese Academy of Sciences, Beijing 100049, China*

Abstract

The ion motions in a Penning trap have been studied in detail in the presence of azimuthal dipolar and quadrupolar radio-frequency excitations and buffer gas cooling. The numerical solutions by using the Runge-Kutta method and thus the pictures of the ion trajectories in the trap have been obtained for different cases and summarized in graphical form. For the recentering of the ion of interest and to perform the purification of the ion species, one has to set a reasonable buffer gas pressure in the trap and apply azimuthal quadrupolar excitation at frequency $\omega_{rf} = \omega_c$.

Keywords: Ion trap, ion motion, ion trajectory, numerical description, mass measurement

1. Introduction

Penning traps have become very accurate tools for mass determination both on stable and unstable isotopes. There are many Penning traps which are in operation or under construction all over the world, such as ISOLTRAP [1] in CERN, SHIPTRAP [2] in GSI, LEBIT [3] in MSU, CPT [4] in ANL, JYFLTRAP in JYFL [5] and so on. At the Institute of Modern Physics, Chinese Academy of Sciences, the LPT (Lanzhou Penning Trap) is also under construction [6].

In an ideal Penning Trap, an ion is confined by the combination of an electrostatic quadruploar field and a homogeneous magnetic fields, and its motion is a superposition of three eigenmotions, an axial oscillation (z) with frequency ω_z and two radial motions commonly referred as reduced cyclotron (+) and magnetron motions (−) with frequency ω_+ and ω_-, respectively. To measure the ion's mass with high precision, one of the methods is to perform buffer gas cooling and radio-frequency (rf) excitations to remove unwanted ions from nuclear reactions and other sources. This method has been used in many Penning traps.

The ion motion can be driven by oscillating electric fields and this in general results in a change of the amplitudes of the eigenmotions. The effect of the driving field on the ion motion depends on the multipolarity of the field and its frequency. A dipole field at one of the eigenfrequencies can be used to increase the amplitude of the corresponding eigenmotion, and this dipolar excitation at $\omega_{rf} = \omega_-$ is generally a significant step to remove the unwanted ions. If ion is excited by a quadrupolar field with a frequency $\omega_{rf} = \omega_c$, where ω_c is the cyclotron frequency of the ion, the magnetron motion and cyclotron motion will be continuously converted into each other, and this is always used to determine the true value of ω_c. If all three eigenfrequencies are measured, the invariance theorem of Brown and Gabrielse [7] can be used.

Cooling of stored ions results in a reduction of the motional amplitudes, and the cooled ions can be trapped in a much smaller volume and thus probe less of the imperfections in the trapping electric and magnetic fields. The technique of buffer gas cooling is commonly applied for radioactive ions stored in a Penning trap, and noble gases are typically used because of their high ionization potential and thus minimum losses due to charge exchange.

So an ion confined in a Penning trap will experience the forces from both the electrostatic field and the magnetic field, and the effects of rf excitation and buffer gas. The equations of ion motion become very complicated and it is very difficult to solve them analytically without any approximation.

Starting from analytical solution, Bollen et al. [8] described ion trajectories under different excitation scenarios qualitatively and identified the important causes of uncertainty in high-precision mass measurements of heavy ions. Savard et al. [9] presented ion trajectories in Penning traps in the presence of buffer gas from Runge-Kutta integration of the relevant equations of motion and demonstrated experimentally the effect of buffer gas cooling. König et al. [10] investigated the ion motion in the presence of an azimuthal quadrupolar rf field and buffer gas cooling and excellent agreement was observed between theoretical results and experimental data.

In this paper we solve those equations of ion motion numerically by using Runge-Kutta method, obtain the ion trajectories in the trap for many different cases and summarize the ion trajectories in graphical form to help us to understand the physical picture in a Penning trap.

*Corresponding author.
Email addresses: sunyuliang@impcas.ac.cn (Y.L. Sun), huangwx@impcas.ac.cn (W.X. Huang)

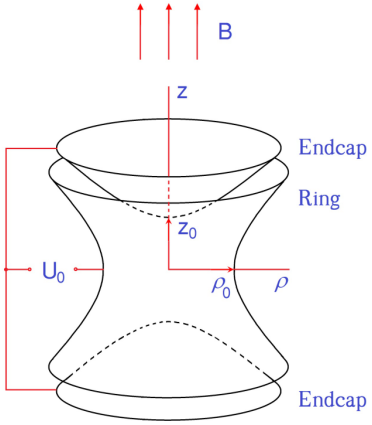

Figure 1: Schematic layout of a typical Penning trap

2. Dynamical equations of ion motion

Figure 1 shows the schematic layout of a typical Penning trap. In an ideal Penning trap a charged particle with a mass of m and a charge of q is confined by the combination of a homogeneous magnetic field $\vec{B} = B\hat{e}_z$ and an axial quadrupolar potential $\Phi(z,\rho) = \frac{U_0}{2d^2}(z^2 - \frac{1}{2}\rho^2)$, where U_0 is the applied trapping voltage between the ring electrode and the two endcap electrodes, d describes the dimension of the trap and is defined by $d = \sqrt{2z_0^2 + \rho_0^2}/2$, where ρ_0 is the inner radius of the ring electrode and $2z_0$ the distance between the endcaps. The forces that the ion in the trap will suffer are:

$$\begin{cases} m\ddot{\vec{z}} = q\vec{E}_z \\ m\ddot{\vec{\rho}} = q(\vec{E}_\rho + \dot{\vec{\rho}} \times \vec{B}), \end{cases} \tag{1}$$

where $\vec{E}_z = -\frac{U_0}{d^2} \cdot z\hat{e}_z$ and $\vec{E}_\rho = \frac{U_0}{2d^2} \cdot \rho\hat{e}_\rho$. Therefore, the axial motion is a harmonic oscillation parallel to the magnetic field with a frequency of

$$\omega_z = \sqrt{\frac{qU_0}{md^2}}, \tag{2}$$

and the radial motion is a superposition of two eigenmotions with frequencies of

$$\omega_\pm = \frac{\omega_c}{2} \pm \sqrt{\frac{\omega_c^2}{4} - \frac{\omega_z^2}{2}}, \tag{3}$$

where

$$\omega_c = \frac{q}{m}B. \tag{4}$$

In order to remove unwanted ions and measure the ion's mass, one method is to perform buffer gas cooling and rf excitations on the ion. Thus the equations of ion motion become more complicated than the ideal case mentioned above.

A dipole field is created by an rf voltage with amplitude V_d and frequency ω_{rf} applied with a phase difference of 180° between two opposite segments of the ring electrode, and it gives an additional electric field [11, 12], for example, for the radial x-component:

$$\vec{E}_x = \frac{V_d}{a}cos(\omega_{rf}t - \phi_{rf}) \cdot \hat{e}_x, \tag{5}$$

where a is the inner radius of the trap. An azimuthal quadrupolar rf field with amplitude V_q and frequency ω_{rf} applied with 180° phase shifts on sets of ring-electrode segments perpendicular to each other gives an additional electric field [10]:

$$\begin{cases} \vec{E}_x = \frac{2V_q}{a^2}cos(\omega_{rf}t - \phi_{rf}) \cdot y\hat{e}_x \\ \vec{E}_y = \frac{2V_q}{a^2}cos(\omega_{rf}t - \phi_{rf}) \cdot x\hat{e}_y, \end{cases} \tag{6}$$

where $\hat{e}_x$ and $\hat{e}_y$ are the unit vectors on the x and y axes, respectively.

Zhu et al. [13] studied the energy limitation for models to simulate the buffer gas cooling and suggested that the viscous drag force model should be used when the ion's energy is less than ~5 eV/u. Thus the effect of the buffer gas on the ion motion in a Penning trap can be described as $\vec{F} = -\delta m\vec{v}$, where δ is the damping parameter describing the effect of the buffer gas. With the ion mobility K_0, δ can be written as $\delta = \frac{q}{m}\frac{1}{K_0}\frac{P/P_N}{T/T_N}$. Here, q/m is the ion's charge-to-mass ratio and P and T are the gas pressure and temperature in units of normal pressure and temperature P_N and T_N [14], respectively.

Thus the dynamical equations including all effects from the dipolar rf excitation and buffer gas cooling can be described as:

$$\begin{cases} \left(\ddot{x} - \frac{qU_0}{2md^2}x - \frac{qB}{m}\dot{y}\right) & -\frac{qV_d}{ma}cos(\omega_{rf}t - \phi_{rf}) & +\delta_x\dot{x} = 0 \\ \left(\ddot{y} - \frac{qU_0}{2md^2}y + \frac{qB}{m}\dot{x}\right) & & +\delta_y\dot{y} = 0 \\ \left(\ddot{z} + \frac{qU_0}{md^2}z\right) & & +\delta_z\dot{z} = 0, \end{cases} \tag{7}$$

and those for the quadrupolar excitation and buffer gas cooling:

$$\begin{cases} \left(\ddot{x} - \frac{qU_0}{2md^2}x - \frac{qB}{m}\dot{y}\right) & -\frac{2qV_q}{ma^2}cos(\omega_{rf}t - \phi_{rf}) \cdot y & +\delta_x\dot{x} = 0 \\ \left(\ddot{y} - \frac{qU_0}{2md^2}y + \frac{qB}{m}\dot{x}\right) & -\frac{2qV_q}{ma^2}cos(\omega_{rf}t - \phi_{rf}) \cdot x & +\delta_y\dot{y} = 0 \\ \left(\ddot{z} + \frac{qU_0}{md^2}z\right) & & +\delta_z\dot{z} = 0. \end{cases} \tag{8}$$

Here, the first part describes the ion motion in an ideal Penning trap, the second is from the dipolar/quadrupolar rf electric field and the third is from the buffer gas.

As these are nonlinear differential equations, an analytic solution is difficult to obtain, and the method which has been known is using variable substitution twice ($\vec{V}^{\pm}(t) = \dot{\vec{\rho}}(t) - \omega_{\mp}\vec{\rho}(t) \times \hat{e}_z, \vec{A}_{\pm}(t) = \vec{V}^{\pm}(t)e^{\mp i(\omega_{\pm}t + \phi_{\pm})}$) and neglecting the high frequency terms [8, 10]. Here we obtain the numerical solution of the above equation by using Runge-Kutta method.

3. Numerical solution by the Runge-Kutta method

Common fourth-order Runge-Kutta method is used to obtain the numerical solution of ion motions in a Penning trap. Specifying the form of first order differential equation as $y'(t) = f(t,y)$ and defining its initial value as $y(t_0) = y_0$, the following equations are introduced:

$$\begin{cases} y_{k+1} = y_k + \frac{h(f_1+2f_2+2f_3+f_4)}{6} \\ t_{k+1} = t_k + h, \end{cases} \tag{9}$$

Table 1: Parameters used in the calculation

h(s)	B(T)	U_0(V)	d(mm)	a(mm)	m(u)	P(Pa)
1×10^{-8}	6.95	100	25.84	16	200	5

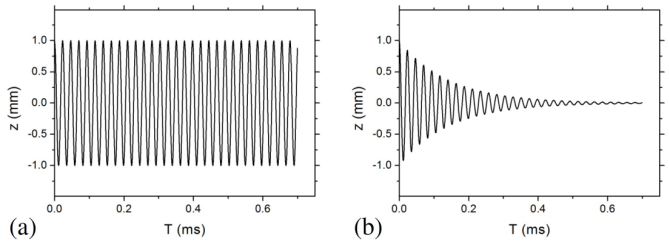

Figure 2: Axial ion trajectories in a plane along the magnetic field as a function of elapsed time. (a) without buffer gas; (b) with helium buffer gas at a pressure of 5 Pa.

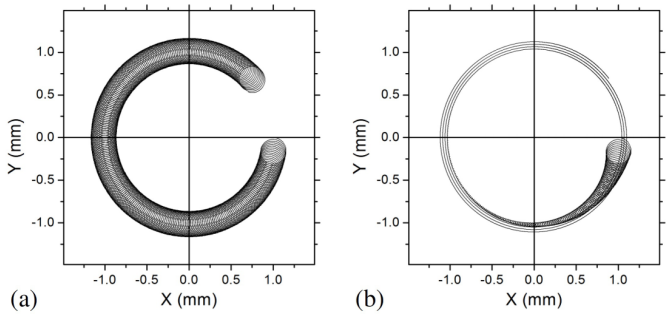

Figure 3: Radial ion trajectories in a plane perpendicular to the magnetic field without excitation. The trap center is at the point (0, 0) marked as a cross, and the ion starts at the point (1.0 mm, 0.0 mm). (a) without buffer gas; (b) with helium buffer gas at a pressure of 5 Pa. Note that the ion moves in a clockwise direction.

where h is the time interval, y_{k+1} is the approximation of $y(t_{k+1})$ and

$$\begin{cases} f_1 = f(t_k, y_k) \\ f_2 = f(t_k + \frac{h}{2}, y_k + \frac{h}{2} f_1) \\ f_3 = f(t_k + \frac{h}{2}, y_k + \frac{h}{2} f_2) \\ f_4 = f(t_k + h, y_k + h f_3). \end{cases} \tag{10}$$

Studies show that the error per step is on the order of h^5, while the total accumulated error has order h^4 [15, 16]. Four slopes corresponding to each dependent variable need to be calculated by the same method mentioned above. The equations (7) and (8) can be rewritten as first order differential equations by defining new variables $x1 = \dot{x}$ and $y1 = \dot{y}$.

Table 1 shows some parameters used in the calculation. A proper value of interval h was chosen to reduce the accumulated error and running time for the calculation. The parameters B, U, d and a in the LPT [6, 17] are used. In order to show the effect of excitation clearly, larger values have been chosen for V_d, the driving rf amplitude for dipolar excitation, V_q, that for quadrupolar excitation and P, the helium buffer gas pressure for cooling. The trajectories of ion with mass 200 have been obtained for many different cases.

3.1. Axial motion

Figure 2(a) shows the ion trajectory in axial direction along the magnetic field without the presence of buffer gas. It is a harmonic oscillation with frequency ω_z and can be obtained from the analytic solution of equation (1). But with the presence of buffer gas, it is difficult to get the analytic solution without approximation. The numerical solution (figure 2(b)) shows that the ion will experience a damped vibration and the distance from the center of the trap will get smaller and smaller. Finally, the ions will be concentrated very close to the center of the trap.

3.2. Radial motion without excitation

In an ideal trap without the electric field for excitations and without the presence of buffer gas, the radial motion is a superposition of reduced cyclotron motion with frequency ω_+ and magnetron motion with frequency ω_-. The ion trajectory is shown in figure 3(a). The radius of cyclotron motion depends on the initial velocity of the ion, the greater the initial velocity, the larger the cyclotron radius. The radius of magnetron motion depends on the initial distance from the trap center, and a further distance makes a lager radius of the magnetron motion. Without the presence of buffer gas, the cyclotron and magnetron motions of the ion will keep its initial status. But with the buffer gas, the cyclotron motion will be damped and the magnetron motion will increase steadily but slowly, as shown in figure 3(b).

3.3. Radial motion with azimuthal dipolar excitation

The phase of the exciting dipolar rf field with respect to the initial magnetron motion has a very strong effect on the magnetron radius [11, 12]. Depending on this phase difference one may actually decrease the magnetron radius. In all the calculations shown in this section, we choose the phase difference as the most favorable value to enhance the magnetron radius.

Figure 4(a) and (b) show the ion trajectories in radial direction when the azimuthal dipolar excitation is applied at $\omega_{rf} = \omega_-$, for the cases without and with buffer gas cooling, respectively. The buffer gas has no obvious effect on the magnetron motion and its amplitude increases continuously. Moreover, all ions can be driven to a larger radius by this azimuthal dipolar excitation, because the first-order approximation of ω_- is independent of the ion's mass. For the cyclotron motion, its amplitude becomes smaller and smaller when the buffer gas is present.

Figure 4(c) and (d) show the similar results as figure 4(a) and (b), but with the applied dipolar excitation at $\omega_{rf} = \omega_+$. Clearly, the dipolar field drives the cyclotron motion and the magnetron motion keeps constant without the presence of buffer gas. But with the buffer gas, the amplitude of the cyclotron motion is damped and that of the magnetron motion increases slowly and continuously.

When the dipolar excitation is applied at frequencies other than ω_- and ω_+, the picture is not very simple because other sidebands, for example, $2\omega_-$ and $2\omega_+$, may occur. However, if the excitation is performed at frequencies other than those particular values, the field doesn't drive the cyclotron or magnetron motion and it almost has no effect on the ion trajectories. The

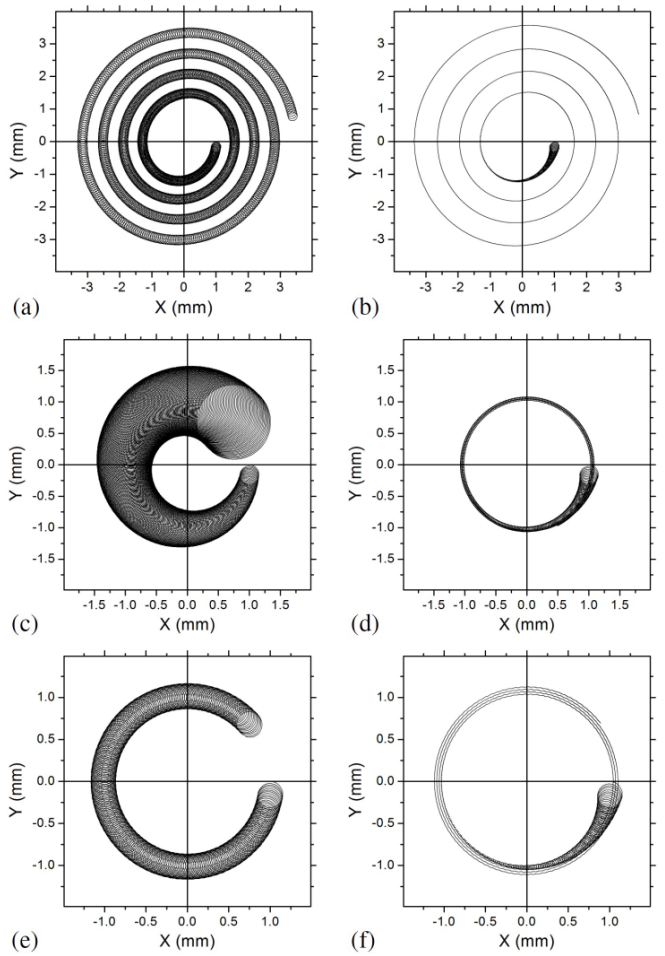

Figure 4: Same as figure 3, but with azimuthal dipolar excitation. The left panels are obtained without buffer gas, and the right panels are with helium buffer gas at a pressure of 5 Pa. (a) and (b): $\omega_{rf} = \omega_-$; (c) and (d): $\omega_{rf} = \omega_+$; (e) and (f): $\omega_{rf} \neq \omega_-$, ω_+ or other sidebands. Note that the ion moves in a clockwise direction.

ion trajectories shown in figure 4(e) and (f) are very similar to those (figure 3) obtained without any excitation.

3.4. Radial motion with azimuthal qradrupolar excitation

Figure 5 shows the ion trajectories in radial direction when the azimuthal quadrupolar excitation is applied at the resonant mode, $\omega_{rf} = \omega_c = \omega_+ + \omega_-$, and at the non-resonant mode, $\omega_{rf} \neq \omega_c$, for the cases without and with buffer gas cooling. Initially there is only magnetron motion.

Without the presence of buffer gas, the two eigenmotions are coupled and a full periodic conversion between the two motions is obtained after a certain time (depending on the amplitude V_q of the excitation). For non-resonant excitation, the conversion is not complete. By scanning the frequency of this quadrupolar excitation, the coupled cyclotron frequency can be obtained by using the time-of-flight ion cyclotron resonance (TOF-ICR) detection technique [18] and then the mass of the ion can be calculated by using equation (4). This is typically used for the mass measurement in most of the Penning traps around the world.

When the buffer gas is present in the trap, the behaviour of the ion becomes quite different. When in resonance, if reasonable buffer gas pressure is applied, both the cyclotron and magnetron motions decrease as a function of time and eventually the ion will go back to the center of the trap. On the contrary, when out of resonance, the ion will keep moving at the larger orbit and never go back to the center. Thus, this mass-selective centering can be used to purify the ion species and the contaminations will be lost by using a very small pore during the transportation of the ions.

In fact, when in resonance, the decrease of the motional amplitudes as a function of time depends heavily on the damping constant. This has not been studied in detail and thus overlooked in the previous research papers. Figure 6 shows the ion trajectories in radial direction when the azimuthal quadrupolar excitation is applied at the resonant mode with different buffer gas pressures. When the buffer gas pressure in the trap is too low (Figure 6(a)), some periodic conversion could still occur as the gas can not cool the ion fast enough. As the pressure goes higher and higher, the ion can be cooled faster and faster, and both the cyclotron and magnetron motions then decrease as a function of time and eventually the ion will go back to the center of the trap (Figure 6(c)). But if the buffer gas pressure is too high then the increase in magnetron radius becomes significant, and the ion will never go back to the center (Figure 6(e)). So if one wants to use this method to recenter the ion of interest and purify the ion species, one has to set a reasonable buffer gas pressure.

Figure 7 shows the centering time as a function of helium buffer gas pressure P and driving rf amplitude V_q for azimuthal quadrupolar excitation. All excitations are performed at $\omega_{rf} = \omega_c$ and all ions start at the point (1.0 mm, 0.0 mm). The centering time is defined as the time-of-flight when the distance between the ion's position and the trap center has decreased to less than 0.1 mm for 0.1 ms, which we consider the ion has been recentered. Obviously, to obtain a shorter centering time, one has to find a reasonable combination of P and V_q. In our calculation, when different buffer gases, such as helium, neon, and argon, are used, the corresponding shortest centering times have been obtained to be 0.36 ms at ~10 Pa and ~28 V, 0.53 ms at ~5 Pa and ~28 V, and 0.90 ms at ~0.5 Pa and ~16 V, respectively. As heavier buffer gas is used, the optimal gas pressure becomes lower, maybe due to the increase of the stopping power. For a lower buffer gas pressure, the centering time becomes longer, but too much buffer gas makes the ion move to the larger radius. For the driving rf field, its amplitude also affects the centering time, but we can not apply a very high amplitude practically in a real experiment, since it distorts the electrical field in the trap too much. So, to obtain a reasonable centering time in a real experiment, we recommend that the helium gas pressure should be set in the range of 0.01 – 5 Pa and the driving rf amplitude for quadrupolar excitation should be set in the range of 2 – 15 V.

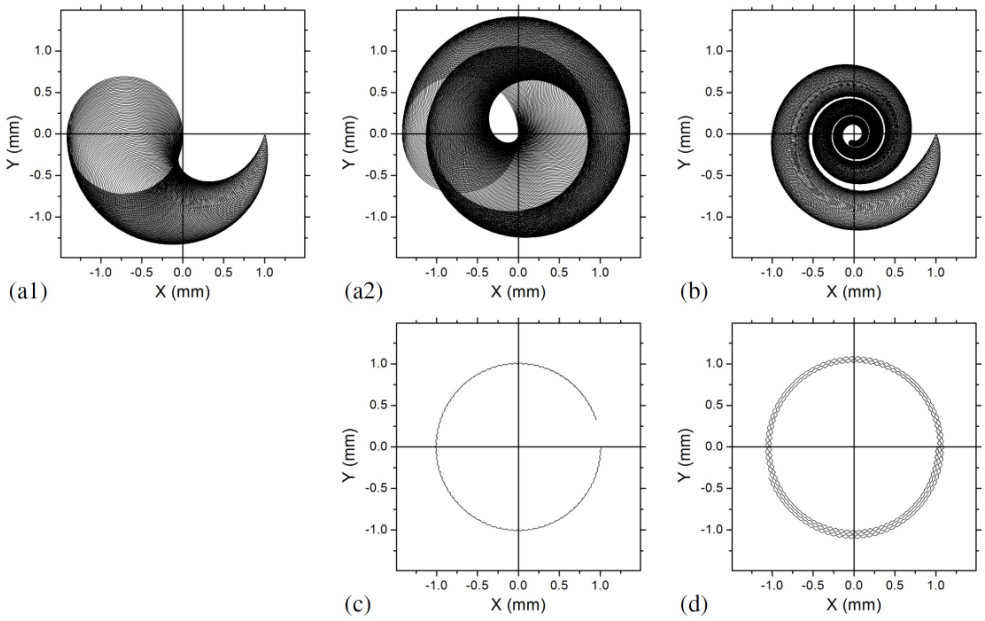

Figure 5: Same as figure 3, but with azimuthal quadrupolar excitation. Initially there is only magnetron motion. The left and middle panels are obtained without buffer gas, and the right panels are with helium buffer gas at a pressure of 5 Pa. (a) and (b): $\omega_{rf} = \omega_c$; (c) and (d): $\omega_{rf} \neq \omega_c$. (a1) and (a2) show the first and second half of the conversion. Note that the ion moves in a clockwise direction.

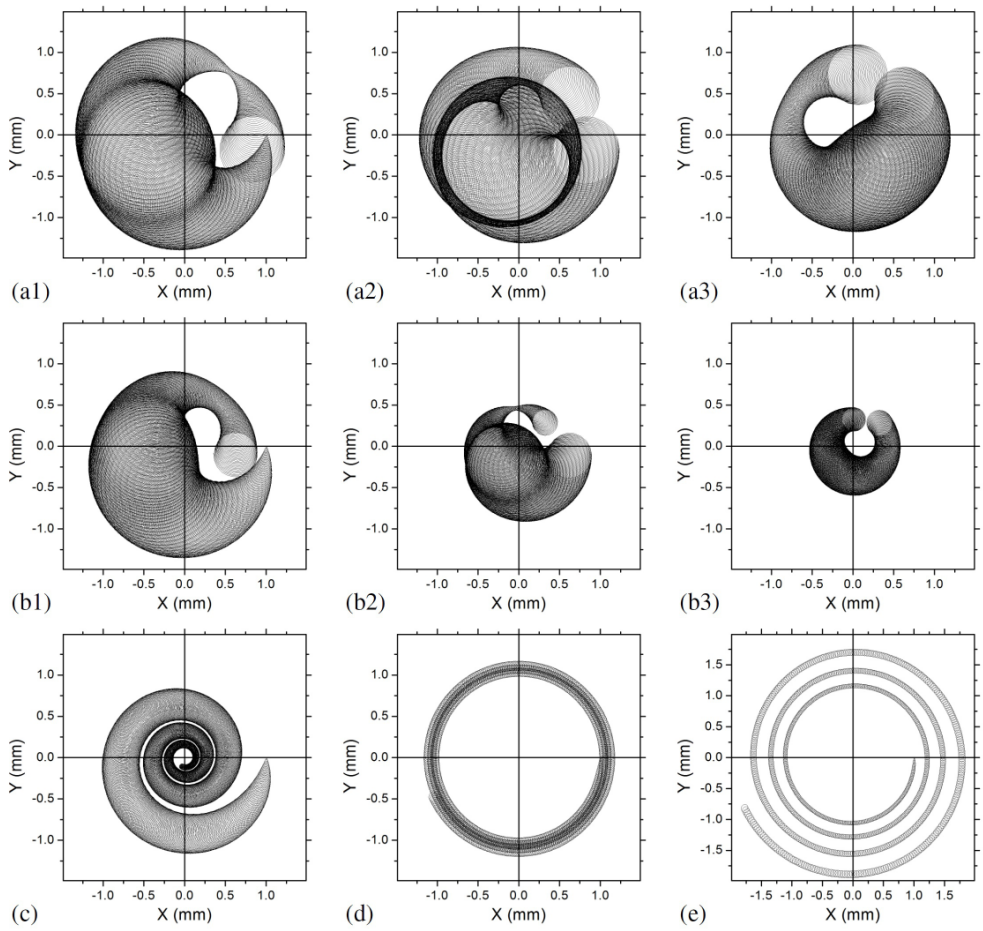

Figure 6: Same as figure 3, but with azimuthal quadrupolar excitation at $\omega_{rf} = \omega_c$ and with helium buffer gas at pressures of (a) 0.05 Pa, (b) 0.5 Pa, (c) 5 Pa, (d) 30 Pa and (e) 50 Pa. Initially there is only magnetron motion. (a1)–(a3) and (b1)–(b3) show successively the ion trajectories with helium buffer gas at pressures of 0.05 Pa and 0.5 Pa, respectively. Note that the ion moves in a clockwise direction.

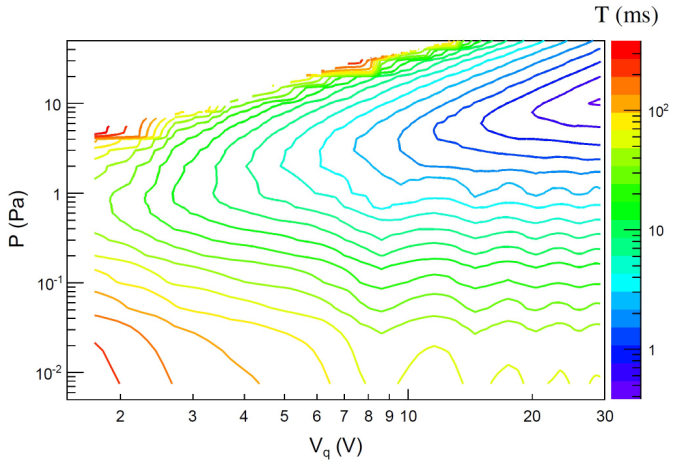

Figure 7: (color online) The centering time T as functions of helium buffer gas pressure P and driving rf amplitude V_q for azimuthal quadrupolar excitation. All excitations are performed at $\omega_{rf} = \omega_c$.

4. Summary

Penning traps have become very accurate tools for mass determination both on stable and unstable isotopes. In order to manipulate the ions in the trap, azimuthal dipolar and quadrupolar rf excitations and buffer gas cooling have to be applied, thus the ion motions become very complicated and the analytic solutions are impossible to obtain without approximation. We have studied in detail the numerical solutions of the ion motions by using the Runge-Kutta method for the different cases which can be used in the experiments for high precision mass measurements. The ion trajectories in the trap for those different cases have been obtained and summarized in graphical form.

Ion motion in the trap depends heavily on the multipolarity of the rf field, its frequency and the buffer gas pressure. Azimuthal dipolar excitation at frequency $\omega_{rf} = \omega_-$ can be used to drive all the ions to a larger radius. Azimuthal quadrupolar excitation at frequency $\omega_{rf} = \omega_c$ without the presence of buffer gas in the trap is generally used to measure the mass of the ion. For the recentering of the ion of interest and to perform the purification of the ion species, one has to set a reasonable buffer gas pressure in the trap and apply quadrupolar excitation at frequency $\omega_{rf} = \omega_c$.

Acknowledgements

This work is supported by Chinese Academy of Sciences, National Natural Science Foundation of China (Grant Nos: 10627504, 11075188), and Major State Basic Research Development Program of China (Contract No. 2013CB834400).

[1] G. Bollen, S. Becker, H.J. Kluge, M. Konig, R.B. Moore, T. Otto, H. Raimbault-Hartmann, G. Savard, L. Schweikhard, H. Stolzenberg, Nucl. Instr. Meth. A 368 (1996) 675.

[2] G. Sikler, D. Ackermann, F. Attallah, D. Beck, J. Dilling, S.A. Elisseev, H. Geissel, D. Habs, S. Heinz, F. Herfurth, F. Heberger, S. Hofmann, H.J. Kluge, C. Kozhuharov, G. Marx, M. Mukherjee, J. Neumayr, W.R. Pla, W. Quint, S. Rahaman, D. Rodriguez, C. Scheidenberger, M. Tarisien, P. Thirolf, V. Varentsov, C. Weber, Z. Zhou, Nucl. Instr. Meth. B 204 (2003) 482.

[3] G. Bollen, S. Schwarz, D. Davies, P. Lofy, D. Morrissey, R. Ringle, P. Schury, T. Sun, L. Weissman, Nucl. Instr. Meth. A 532 (2004) 203.

[4] J.C. Wang, G. Savard, K.S. Sharma, J.A. Clark, Z. Zhou, A.F. Levand, C. Boudreau, F. Buchinger, J.E. Crawford, J.P. Greene, S. Gulick, J.K.P. Lee, G.D. Sprouse, W. Trimble, J. Vaz, B.Z. Zabransky, Nucl. Phys. A 746 (2004) 651.

[5] V.S. Kolhinen, S. Kopecky, T. Eronen, U. Hager, J. Hakala, J. Huikari, A. Jokinen, A. Nieminen, S. Rinta-Antila, J. Szerypo, J. Äysto, Nucl. Instr. Meth. A 528 (2004) 776.

[6] W.X. Huang, Y.L. Tian, Y. Wang, J.Y. Wang, Z.C. Zhu, Y.L. Sun, W. Wei, H. Yuan, L.Z. Ma, H.S. Xu, G.Q. Xiao, Plasma Science & Technology 14 (2012) 421.

[7] L.S. Brown, G. Gabrielse, Rev. Mod. Phys. 58 (1986) 233.

[8] G. Bollen, R.B. Moore, G. Savard, H. Stolzenberg, J. Appl. Phys. 68 (1990) 4355.

[9] G. Savard, S. Becker, G. Bollen, H.J. Kluge, R.B. Moore, T. Otto, L. Schweikhard, H. Stolzenberg, U. Wiess, Phys. Lett. A 158 (1991) 247.

[10] M. König, G. Bollen, H.-J. Kluge, T. Otto, J. Szerypo, Int. J. Mass Spectrom. 142 (1995) 95.

[11] K. Blaum, Phys. Rep. 425 (2006) 1.

[12] K. Blaum, G. Bollen, F. Herfurth, A. Kellerbauer, H.J. Kluge, M. Kuckein, S. Heinz, P. Schmidt, L. Schweikhard, J. Phys. B 36 (2003) 921.

[13] Z.C. Zhu, W.X. Huang, Y.L. Sun, Y. Wang, Y.L. Tian, J.Y. Wang, Int. J. Mass Spectrom. 309 (2012) 44.

[14] E.W. McDaniel and E.A. Mason, The Mobility and Diffusion of Ions in Gases, Wiley, New York, 1973.

[15] U.M. Ascher and L.R. Petzold, Computer Methods for Ordinary Differential Equations and Differential-Algebraic Equations, Society for Industrial and Applied Mathematics, Philadelphia, 1998.

[16] J.C. Butcher, Numerical Methods for Ordinary Differential Equations, John Wiley & Sons, New York, 2003.

[17] W.X. Huang, J.Y. Wang, Y. Wang, Y.L. Tian, Z.C. Zhu, H.S. Xu, G.Q. Xiao, Chin. Phys. C 33 (S1) (2009) 193.

[18] G. Gräff, H. Kalinowsky and J. Traut, Z. Phys. A 297 (1980) 35.